Available online at www.sciencedirect.com

SCIENCE DIRECT®

Virology 321 (2004) 144–153

VIROLOGY

www.elsevier.com/locate/yviro

The M1 matrix protein controls the filamentous phenotype of influenza A virus

C.J. Elleman and W.S. Barclay*

School of Animal and Microbial Sciences, University of Reading, Whiteknights, Reading RG6 6AJ, UK

Received 7 July 2003; returned to author for revision 3 December 2003; accepted 9 December 2003

Abstract

We show that most isolates of influenza A induce filamentous changes in infected cells in contrast to A/WSN/33 and A/PR8/34 strains which have undergone extensive laboratory passage and are mouse-adapted. Using reverse genetics, we created recombinant viruses in the naturally filamentous genetic background of A/Victoria/3/75 and established that this property is regulated by the M1 protein sequence, but that the phenotype is complex and several residues are involved. The filamentous phenotype was lost when the amino acid at position 41 was switched from A to V, at the same time, this recombinant virus also became insensitive to the antibody 14C2. On the other hand, the filamentous phenotype could be fully transferred to a virus containing RNA segment 7 of the A/WSN/33 virus by a combination of three mutations in both the amino and carboxy regions of the M1 protein. This observation suggests that an interaction among these regions of M1 may occur during assembly.

Keywords: Influenza; Filament; Reverse genetics

Introduction

Influenza virus particles can display different morphologies. Some isolates form long filaments up to several micrometers long as they emerge from the cell, but other well-studied laboratory-adapted strains produce 100-nm spherical particles (Cox et al., 1980; Roberts and Compans, 1998; Smirnov et al., 1991). This implies that viral and host cell factors may influence virus morphology, and that some of the mutations that adapt virus for growth in different substrates may concomitantly result in morphological changes.

Below the host-derived lipid bilayer that forms the envelope of the influenza A virus particle lies a layer of matrix protein, M1. This is the most abundant protein of the virion, and it possesses both nucleic acid and membrane binding activity (Bucher et al., 1980; Wakefield and Brownlee, 1989). The M1 protein is encoded by RNA segment 7 which also encodes a small ion channel protein, M2, by using an alternative splicing strategy (Inglis and Brown, 1981; Lamb and Choppin, 1981). Expression of M1 protein alone can drive budding of vesicles from the plasma membrane (Gomez-Puertas et al., 2000; Latham and Galarza, 2001) and this observation implies that M1 exerts a driving force for virus assembly and release.

Evidence that the gene products of RNA segment 7, namely, M1 and M2 proteins, play a role in influenza A virus assembly comes from studies with an M2 specific monoclonal antibody, 14C2. This antibody binds an epitope present in the ectodomain of many strains of influenza A virus M2 but reduces infectivity of just a subset of them (Zebedee and Lamb, 1988). Influenza strain A/Udorn/72, which readily forms filamentous virions, was used to select for mutant viruses that displayed resistance to growth inhibition by 14C2. Some of these mutants showed genetic changes in M2, either in the antibody epitope in the ectodomain, or even in the cytoplasmic domain, while other mutants had single amino acid changes such as V31I or V41A in the M1 protein (Zebedee and Lamb, 1989). Interestingly, later studies showed that the mutant viruses altered in M2 retained their filamentous morphology but

* Corresponding author. School of Animal and Microbial Sciences, University of Reading, Whiteknights, PO Box 228, Reading RG6 6AJ, UK. Fax: +44-1189-316671.

E-mail address: w.s.barclay@reading.ac.uk (W.S. Barclay).

0042-6822/$ - see front matter © 2004 Elsevier Inc. All rights reserved.
doi:10.1016/j.virol.2003.12.009

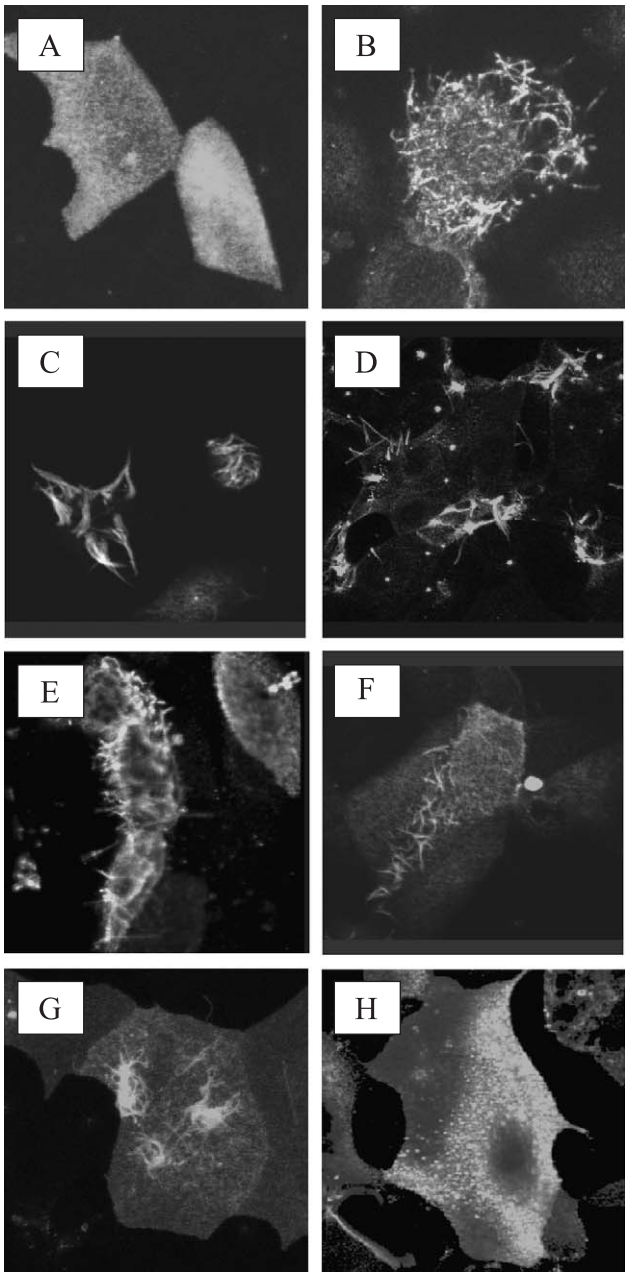

Fig. 1. Induction of filamentous changes at the surface of MDCK cells infected with influenza A viruses. Cells were infected with influenza A virus strains at an moi of 0.1–1 and fixed 24 h after infection with paraformaldehyde. Viral antigen was stained using an antibody to either H3 (polyclonal) or H1 (monoclonal) HA protein. Imaging was carried out on Leica confocal microscope and all images are maximum projections. (A) A/WSN/33 (H1N1); (B) A/Udorn/72 (H3N2); (C) A/England/41/72 (H3N2); (D) A/PortChalmers/73 (H3N2); (E) A/Scotland/52/92 (H1N1); (F) A/Johannesburg/95 (H3N2); (G) A/Victoria/3/75 (H3N2); (H) A/PR8/34 (H1N1).

those changed in M1 now produced predominantly spherical particles (Roberts et al., 1998). Thus, specific sequences in the M1 gene appear to control virus shape.

More recently, a reverse genetics approach has been applied to the analysis of the role of M1 gene in determining influenza morphology (Bourmakina and Garcia-Sastre, 2003). Chimeric and mutant viruses containing Udorn segment 7 RNAs were analyzed for morphology and the results implied a critical role for amino acids at positions 95 and 204 in M1 in filamentous particle formation. Because many traits of influenza viruses have been previously been shown to be multigenic and may be affected by the genetic background of the 'parent virus' used in a particular study, it is important to perform genetic analyses in the context of different strains and subtypes of influenza A virus. We have used a similar approach to the above study but have generated mutant viruses in a different genetic background and here we describe results that subtly differ from those previously reported. This implies that other RNA segments may have a critical influence on morphology. Clearly, the assembly of influenza virus is a complex process dependent on several virus and host cell genes.

Results

Filamentous morphology is independent of subtype and is the common phenotype for human influenza viruses

We obtained a panel of human influenza A virus isolates and analyzed whether they induced filamentous changes on the surface of infected cells. Some of the panel members had not been passaged in eggs, whereas others, such as the A/PR8/34, A/WSN/33, A/Udorn/72, and A/Victoria/3/75 strains had an extensive egg passage history. The panel contained strains of the H1N1 subtype as well as of H3N2.

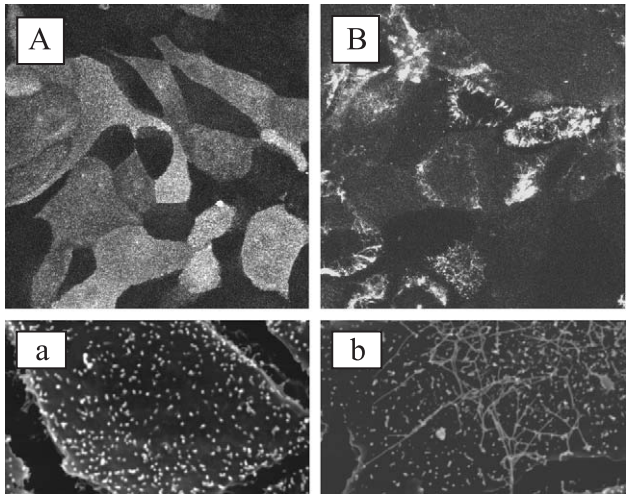

Fig. 2. Cell surface changes in MDCK cells infected with recombinant A/Victoria/3/75 viruses with altered RNA segment 7. MDCK cells were infected with recombinant influenza A viruses at an moi of 1. Twenty-four hours later, they were analyzed by immunofluorescent staining and confocal microscopy (A and B), or by scanning electron microscopy (a and b) for cell surface changes induced by infection. (A and a) Recombinant virus W/V. (B and b) Recombinant virus Ud/V.

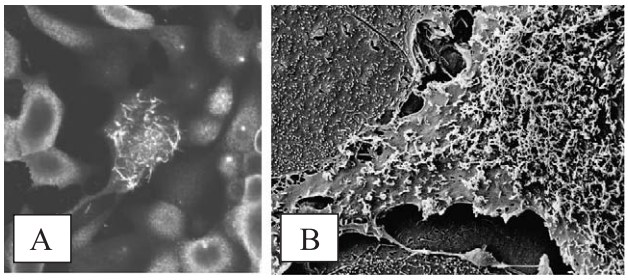

Fig. 3. Filamentous changes are not seen in all infected cells. MDCK cells were infected with recombinant virus UdM1. (A) Immunofluorescence of cell surface viral antigens visualized by confocal microscopy 24 h after infection at moi of 1. (B) Scanning electron microscopy of infected cell monolayer 24 h after infection at moi of 1.

Fig. 1 is a sample of the data obtained which illustrates that the majority of strains formed filaments in a proportion of the infected MDCK cells (Fig. 1, panels B, C, D, E, F, and G). In contrast, cells infected with the A/WSN/33 or A/PR8/34 strains rarely display this appearance (Fig. 1, panels A and H). This implies that the idea that influenza viruses form exclusively 100-nm-diameter spherical particles has arisen from the extensive experimental use of the A/WSN/33 and A/PR8/34 strains.

RNA segment 7 confers filamentous morphology

We employed a reverse genetic approach to investigate the genetic basis of viral filament formation. Previous data had implied a role for the M1 gene in this phenotype. We therefore analyzed the effect of manipulating the M1 gene within a genetic background, which supported filament formation, A/Victoria/3/75 (Fig. 1G). Two single-gene reassortants were rescued entirely from plasmid cDNAs and designated Ud/V and W/V. Ud/V contains the A/Udorn/72 segment 7 in the A/Victoria/3/75 genetic background, while W/V contains the A/WSN/33 segment 7 also in the Victoria background. The surfaces of MDCK cells infected with the two recombinant viruses were analyzed by confocal microscopy (Figs. 2A and B). Cells infected with the Ud/V recombinant produced many long surface filaments while most of those infected with the

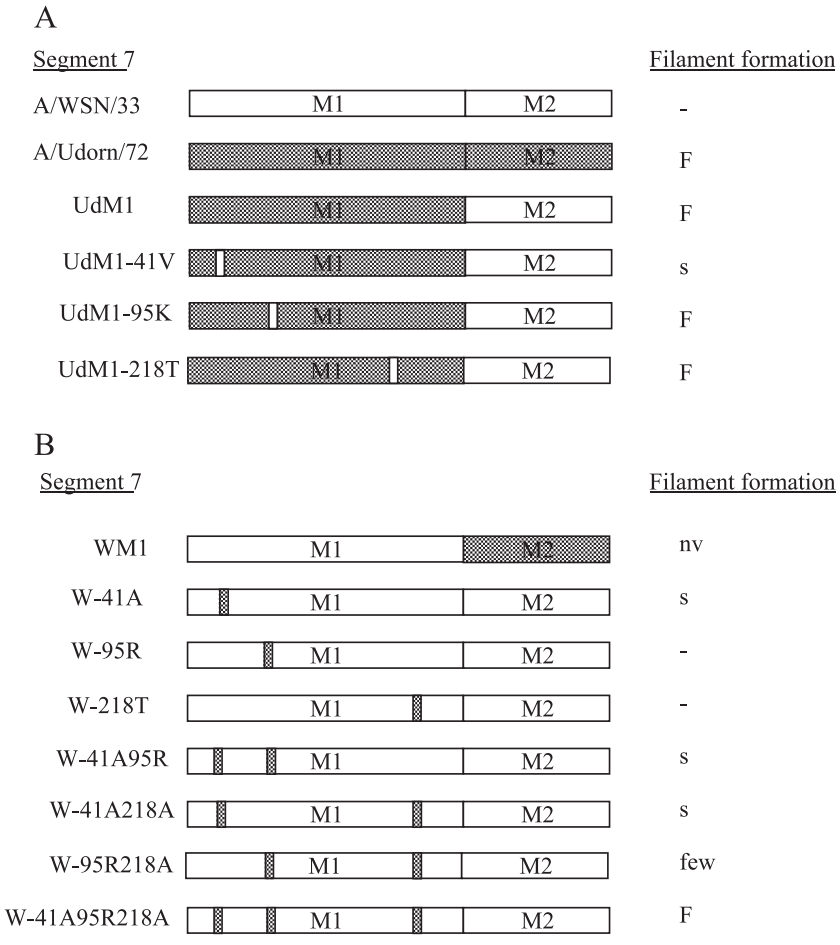

Fig. 4. Mutant segment 7 cDNA introduced into recombinant viruses in this study. (A) Recombinants based on Udorn M1 sequence. (B) Recombinants based on A/WSN/33 segment 7. Shaded areas indicate sequences derived from A/Udorn/72 segment 7, white areas have A/WSN/33 sequences. F, virus induces many long filaments on infected cells; –, virus does not induce filaments on infected cells; s, virus induces short filaments on infected cells; few, virus induces filaments on a few cells; nv, no virus rescued from this construct.

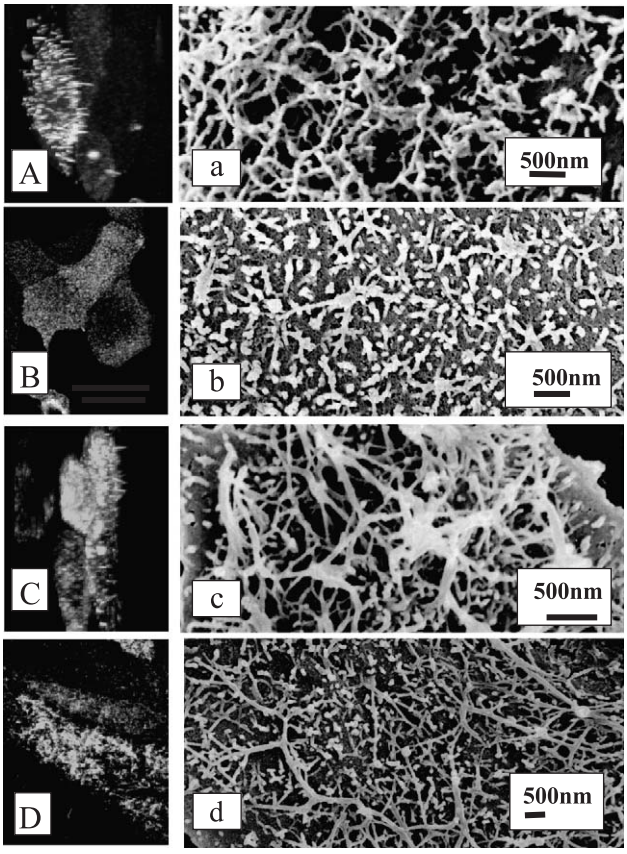

Fig. 5. Fluorescent and SEM micrographs of recombinant viruses to study loss of filamentous phenotype. MDCK cells were infected with recombinant viruses at moi = 1 and analyzed 24 h later by immunofluorescent staining for viral antigen. (A and a) Recombinant virus UdM1. (B and b) Recombinant virus UdM1-41V. (C and c) Recombinant virus UdM1-95K. (D and d) Recombinant virus UdM1-218T.

WSN/V did not. The filaments were also visualized using scanning electron microscopy (Figs. 2a and b), which also allowed clear visualization of long filaments extruding from cells infected with virus with Udorn segment 7 RNA. Interestingly, both confocal analysis and scanning electron microscopy showed that although many of the cells infected with viruses with Udorn RNA segment 7 did produce filaments, others, although infected, did not (Figs. 3A and B). Plaque-purified virus preparations also only induced filamentous changes in a proportion of the cells they infected (data not shown), suggesting that this observation is not due to heterogeneity in the virus preparation.

The M1 gene determines viral morphology

To determine which of the gene products of RNA segment 7 was important for determining virus morphology, chimeric cDNAs were generated which contained mixtures of M1 and M2 proteins from a filamentous and a spherical strain. A recombinant virus was recovered containing a chimeric segment 7 RNA in which the M2 gene of A/Udorn/72 was exchanged for that of A/WSN/33 (Fig. 4A). This virus, designated UdM1, induced a highly filamentous appearance in infected cells (Figs. 5A and a). A reciprocal chimeric virus in which segment 7 contained the A/WSN/33 M1 gene and the A/Udorn/72 M2 gene, WM1, was not rescued, although both M1 and M2 proteins were expressed in the primary transfected cells (data not shown). This suggests that this combination of matrix gene sequences is incompatible.

Our next approach was to map individual residues in the M1 gene which contribute to the filamentous phenotype. For this purpose, we took advantage of the two 'parental' viruses described above, W/V and UdM1, which both encoded the WSN M2 protein and thus differed only in M1 sequence. This allowed us to study the role of M1 residues in an otherwise completely isogenic background.

The amino acids at positions 41, 95, and 218 in M1 strongly influence the filamentous phenotype

A comparison of the amino acid sequences of the M1 proteins of the filamentous A/Udorn/72 and A/Victoria/3/75 viruses with that of the spherical A/WSN/33 and A/PR8/34 viruses indicated six residues which differed among them (Table 1). Two residues at positions 204 and 205 were unique to WSN M1. Because PR8 virus did not induce filaments (Fig. 1, panel H), we considered it unlikely that these two residues were dominant determinants of the filamentous phenotype. To confirm this, we cloned the RNA segment 7 of A/PR8/34 virus and introduced it into the A/Victoria/3/75 genetic background by the reverse genetics technique. This virus therefore contains WSN-like sequence in M1 except at residues 204 and 205 where it is Udorn-like. It also did not induce filamentous changes in infected cells (data not shown). Therefore, although a mutation E204D abrogates the filamentous phenotype (Bourmakina and Garcia-Sastre, 2003), the opposite change D204E does not confer filament induction to a virus with WSN-like M1. The M1 database sequences revealed that another residue which differed between Udorn and WSN M1, position 167, often varied among threonine, alanine, or isoleucine, for example, in the strains shown in Fig. 1, all of which induced filaments. On the other hand, M1 sequences of WSN and PR8 viruses differed from those of all other human strains at positions 41, 95, and 218. We attempted to address whether any one of these three amino acid residues

Table 1
Amino acid differences between M1 proteins of spherical (A/PR8/34 and A/WSN/33) and filamentous (A/Udorn/72) influenza A viruses

Virus amino acid position	41	95	167	204	205	218
A/WSN/33	V	K	T	D	I	T
A/PR8/34	V	K	T	E	V	T
A/Udorn/72	A	R	A	E	V	A/V
A/Victoria/3/75	A	R	A	E	V	A

was a determinant of virus morphology by asking if changing any one of these in the UdM1 background abrogated filament formation (Figs. 4A and 5), and also whether introducing any or all of these changes into the WSN background could confer the filamentous phenotype (Figs. 4B and 6).

We first engineered the change A41V in the chimeric segment 7 (UdM1-41V) and rescued recombinant virus with this mutation. This virus no longer formed filaments detected by confocal microscopy (Fig. 5B), although analysis of the surface of cells analyzed by SEM indicated very short extrusions were present (Fig. 5b). In contrast, a change of R to K at position 95 did not affect the ability of UdM1 virus to form filaments (UdM1-95K, Fig. 5, panels C and c). Thirdly, we considered residue 218. Sequencing various clones, we obtained following reverse transcription and PCR of our laboratory stock of A/Udorn/72 indicated that the amino acid at position 218 was either A, as reported in the database, or V. The chimeric virus rescued as UdM1 contained V at this position and was clearly filamentous, whereas the rescued virus Ud/V had A at this position and also strongly induced filaments in infected cells. Thus, either A or V at this position was associated with filamentous viruses but T was found in both WSN and PR8 spherical strains. Therefore, the change, A to T, was engineered into the UdM1 background (UdM1-218T). This virus induced filaments to the same extent as UdM1 (Fig. 5, panel D).

Next, we performed reciprocal changes mutating amino acids within the WSN M1 gene to those found in the Udorn sequence (Fig. 4B). A mutation was engineered in the WSN segment 7 cDNA to produce the single amino acid change at position 41, from V to A. The recovered virus, designated W-41A (Fig. 6, panel A), did produce some filaments on the infected cell surface when analyzed at high magnification, although they were much shorter than those observed for Ud/V and UdM1. When residue 95 was changed from K to R, the phenotype of virus W-95R was indistinguishable from that of a virus with wild-type WSN segment 7 (Fig. 6, panel B). Similarly, mutant W-218A bearing the change threonine to alanine at residue 218 also did not acquire the filamentous phenotype (Fig. 6, panel C).

Lastly, we assessed whether combinations of changes at these three residues were able to confer the filamentous phenotype to a virus with WSN-like segment 7. Each change was engineered in pairs, to create viruses, W-41A-95R, W-41A-218A, and W-95R-218A, and in addition a triple mutant, W-41A-95R-218A, was recovered (Fig. 4B).

None of the double mutant viruses showed a completely filamentous phenotype, although short extrusions were evident on some cells infected with W-41A-95R and W-41A-218A (Fig. 6, panels E and F), and a few cells infected with W-95R-218A displayed filamentous changes (Fig. 6G). However, the triple mutant induced extensive filament formation and was indistinguishable in phenotype from a virus with Udorn segment 7 (Fig. 6, compare panels D and H). This suggests that changes in the amino half and carboxy half of the M1 protein were able to act in concert to affect the virus morphology.

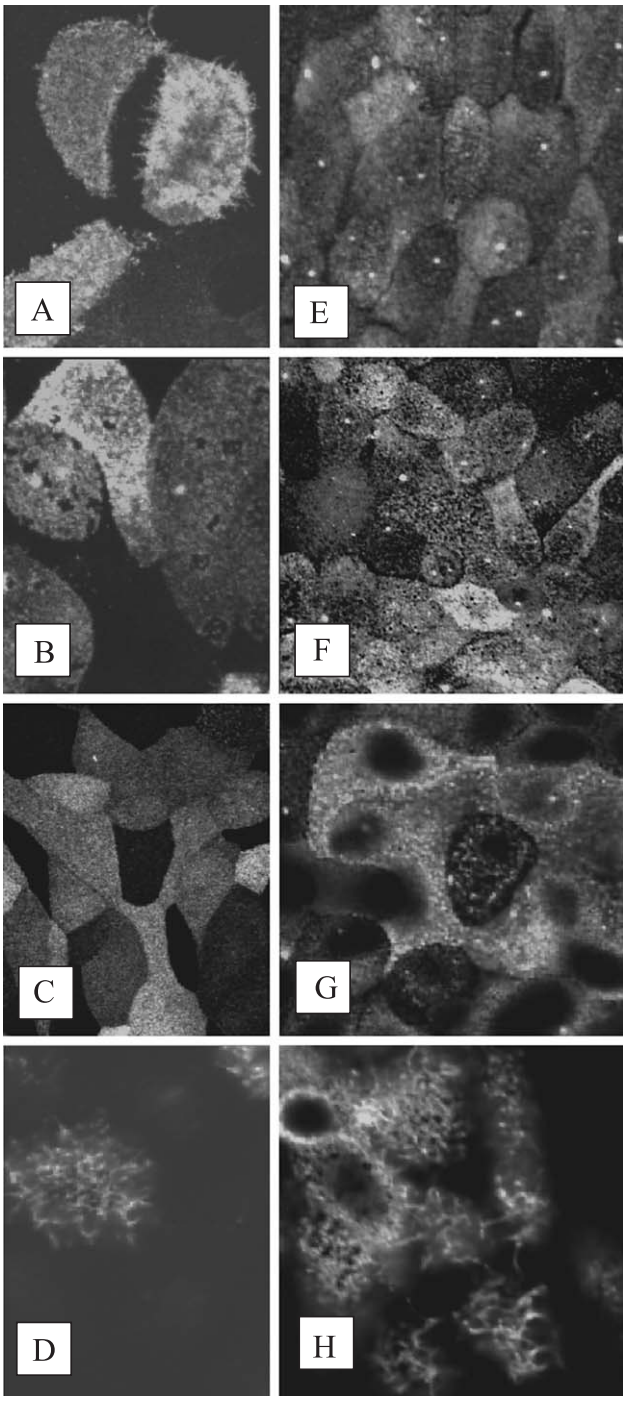

Fig. 6. Fluorescent micrographs of recombinant viruses to show acquisition of filamentous phenotype. MDCK cells were infected with recombinant viruses at moi = 1 and analyzed 24 h later by immunofluorescent staining for viral antigen. Recombinant viruses: (A) W-41A; (B) W-95R; (C) W-218A; (D) UdM1; (E) W-41A-95R; (F) W-41A-218A; (G) W-95R-218A; (H) W-41A-95R-218A.

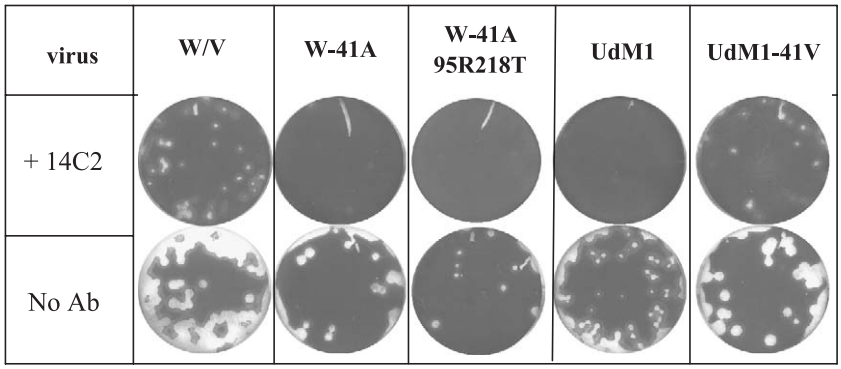

Fig. 7. The effect of antibody 14C2 against M2 on plaque formation by recombinant viruses. Viruses were plaqued in the absence of or presence of 3 μg/ml 14C2 monoclonal antibody and remaining MDCK monolayers were stained after 3 days with crystal violet stain.

14C2 monoclonal antibody inhibition of recombinant viruses which vary in morphology

The sensitivity of recombinant viruses to growth inhibition by the M2 specific antibody 14C2 was determined using a plaque inhibition assay (Fig. 7). The virus with WSN segment 7, W/V, continued to form plaques in the presence of antibody, albeit of a smaller size. However, some derivatives of the W/V virus became sensitive to 14C2 inhibition. Thus, plaque formation by the W-41A mutant was partially inhibited in the presence of 14C2, whereas the triple mutant W-41A-95R-218A failed to produce any plaques in the presence of 3 μg/ml antibody. Conversely, the ability of the UdM1 virus to form plaques was inhibited by 14C2, whereas the UdM1-41V mutant, which contains only one amino acid change from UdM1, produced plaques in both the presence and absence of antibody. We further tested the inhibition of virus production by the 14C2 monoclonal antibody by titrating the yield from infected cells using both infectivity and HA assays (Table 2). Although all viruses were inhibited in the presence of 5 μg/ml antibody, the extent of inhibition varied significantly and in a manner that correlated with the ability to induce filamentous changes on infected cells.

Table 2
Effects of anti-M2 monoclonal antibody 14C2 in virus yields

Virus	Titers released virus in absence/presence of antibody (pfu/ml)	Percentage of yield in absence of antibody	HAU	Fold reduction in HAU
W/V	ND	NA	32/16	2
W-41A	ND	NA	16/2	8
W-95R-218A	ND	NA	16/8	2
W-41A-95R-T218A	ND	NA	16/4	4
Ud/V	$2.8 \times 10^4/1.4 \times 10^3$	5%	2/<2	NA
UdM1	$3.6 \times 10^7/7.7 \times 10^5$	2.1%	16/2	8
UdM1-41V	$2.9 \times 10^4/3.7 \times 10^3$	12.7%	<2/<2	NA

Discussion

The strains of influenza A virus that are commonly studied by most laboratories are the A/WSN/33 and A/PR8/34 strains. Notably, these two strains were the only ones in the present study that did not form filaments. Indeed, our study of a selection of recent isolates showed that the filamentous phenotype is predominant and independent of egg or cell passage or subtype. Other examples of filament formation by recent isolates can be found in the literature (e.g. see Liu et al., 2002). The characteristics of filamentous changes on the infected cell surface varied among strains (compare the appearance of cells in Fig. 1 infected with A/England/42/72, panel C, and A/Port Chalmers/73, panel D, with those infected with A/Johanesburg/95, panel F). These differences may indicate a contribution of other viral genes or of other changes in the M1 gene to the filamentous phenotype. The sequence of the M1 gene of all of the viruses tested in Fig. 1 is not available, but for those which are sequenced, there is some limited but significant variation in M1. Overall, our findings suggest that filament induction is influenced by a constellation of sequences both in M1 and in other viral genes. Thus, our recombinant virus Ud-41V forms only short extrusions on cells, whereas the recombinant W-95R-218A which differs from Ud-41V only at residues 167, 204, and 205 forms clear filaments at least on some cells. We conclude that many different residues in M1 can affect filament induction, and those analyzed here serve to illustrate the ease with which the phenotype can be gained or lost. Moreover, it is clear that other viral genes also affect whether viruses display cell surface filaments or not. Thus, in agreement with earlier work (Roberts et al., 1998; Zebedee and Lamb, 1989), we show here that a single amino acid change from A at residue 41 to V in A/Udorn/72 M1 resulted in a loss of filament production. In contrast, a more recent study (Bourmakina and Garcia-Sastre, 2003) found the A41V change did not abrogate filament formation but the K95R change did. The latter observations were made within the context of the H1N1 A/WSN/33 viral genome, in contrast to our own work, which is based on a genetic

background of the H3N2 A/Victoria/3/75 strain. Changes in influenza RNA segments 4 and 6 which encode HA and NA have been previously shown to result in irregularly shaped virions (Jin et al., 1997; Mitnaul et al., 1996).

In our study, three genetic changes in WSN M1, at amino acids 41, 95, and 218, were required simultaneously to confer fully filamentous phenotype, although changes at residues 95 and 218 also resulted in obvious filament formation. This implies a functional interaction between the two halves of the M1 protein. Both residues 41 and 95 lie on the outer surface of the three-dimensional structure of the amino terminus of M1 (Sha and Luo, 1997). The position of residue 218 is at present unknown as no structure for the C terminus of M1 is available. The M1 protein self-assembles into ribbon-like structures (Harris et al., 2001) and it is possible that the amino acid changes at positions 41, 95, and 218 affect this process. Alternatively, mutations such as those described here might influence the interaction of the hypothetical 'late domain' of M1 (Hui et al., 2003) with a host cell protein which is required for, or which stimulates efficient budding from the plasma membrane. Indeed, the host cell undoubtedly influences the expression of the filamentous phenotype. For example, only polarized cells formed filaments and an intact actin cortex is necessary for filament formation because no filaments were produced in the presence of cytochalasin D (Roberts and Compans, 1998). In the presence of jasplaklinolide, an inhibitor of actin treadmilling, filament formation was disrupted and the plasma membrane distribution of hemagglutinin and other raft-associated proteins profoundly altered (Simpson-Holley et al., 2002). We noted that some cells are reciprocal to filament formation and that this could not be due to genetic heterogeneity in the virus preparation. One explanation for our observations is that cells infected at different stages of their cell cycle may vary in the integrity of their actin cortex and thus their ability to support filaments.

We did not quantify the filamentous phenotype of different mutants in this study. We were not satisfied that methods for quantification used in previous studies would add to our ability to describe the phenotype of a recombinant or isolate. For example, filament quantity and length have been estimated by the deposition of filaments onto TEM grids (Bourmakina and Garcia-Sastre, 2003; Roberts and Compans, 1998). This approach can be problematic because longer filaments either do not attach to the TEM grid or are lost during preparation. Indeed, these authors never showed a filament longer than 3 μm and these were extremely rare. Presumably because of this problem, Bourmakina and Garcia-Sastre (2003) defined a filament as any particle longer 300 nm. However, this is an unrealistic description of the filaments we observe in our studies. In this study, we have been able to describe both long filaments and shorter cell surface extrusions (Figs. 5 and 6) by visualization of the cell surface following immunofluorescent staining. However, because of the variation in filament frequency we observed, a recombinant virus was only designated as filamentous if an equal proportion of infected cells produced filaments clearly visible with the confocal microscope as for the Ud/V-infected control.

Sensitivity of virus to 14C2 inhibition correlated more closely with the filamentous phenotype than with the sequence of the M2 ectodomain which contains the antibody epitope. Thus, the virus UdM1 is sensitive to inhibition by 14C2 antibody although it shares the M2 sequence of the naturally resistant virus WSN. Furthermore, recombinant virus UdM1-41V with an M1 sequence identical to the 1A mutant of Udorn described by Zebedee and Lamb (1989) does not induce filaments and also demonstrated resistance to 14C2. Conversely, viruses with WSN M2 sequence became sensitive to 14C2 if filamentous, even if they only showed short extrusions, for example, W-41A. However, it should be noted that some other previously described 14C2 resistant mutants with changes in M2 (such as the mutant termed 10A (Zebedee and Lamb, 1989) were more filamentous than the wild-type virus (Roberts and Compans, 1998).

We did not rescue a virus with an M1 derived from A/WSN/33 and an M2 from A/Udorn/72, although we could detect that both proteins were produced in transfected cells from the recombinant plasmid. On the other hand, Bourmakina and Garcia-Sastre (2003) did rescue a virus containing this combination of M1 and M2 genes although they used an unnatural coding strategy in their studies by separating M1 and M2 onto different segments, and were also working within the WSN genetic background. Yasuda et al. (1994) were also unable to rescue viruses with particular combinations of M1 and M2. They never obtained a virus with a chimeric segment 7 containing the A/Aichi/68 M1 and A/WSN/33 M2 although they recovered virus with the reverse chimeric segment 7. These data might imply either that a functional match is required between M1 and M2 proteins or that certain RNA sequences are incompatible within segment 7.

The fact that only the WSN and PR8 viruses lack the filamentous phenotype suggests that there has been a selective advantage for the spherical form during the extensive passage history of these strains. The A41V mutation present in both these strains was previously shown to be associated with adaptation of influenza viruses for growth in mice (Ward, 1995). In addition, the high yield cell culture growth characteristics of influenza A virus have previously been attributed to the M1 gene (Yasuda et al., 1993, 1994). A suggestion has been made that the binding of M1 to the RNP is stronger for viruses which grow more efficiently in culture and that this might affect morphology (Liu et al., 2002). Because filamentous viruses are associated with clinical isolates, it is tempting to suggest that there is some advantage in vivo for a virus which can form filaments that is not reflected during mouse passage. Other viruses induce filamentous structures in infected cells. Interestingly, two of these are respiratory pathogens, parainfluenza and respiratory syncytial virus (Brown et al., 2002; Yao and Compans, 2000). In future studies, it will be important to analyze

filamentous viruses under conditions that more nearly represent the situation in their natural habitat, the respiratory tract.

Materials and methods

Cell culture

MDCK cells were used for virus rescue, propagation, and immunofluorescence studies. Cells were maintained in Dulbecco's minimal essential medium supplemented with 20 000 U/l each of penicillin and streptomycin, 5 ml of 2 mM L-glutamine, 1× essential amino acids, and 10% heat-inactivated fetal calf serum. Cells were passaged every 4–5 days in 75-ml flasks. For the transfection step of the virus rescue, 293T cells were used. These were passaged as above using the same media. The day before transfection, 293Ts were seeded into 12-well plates so as to be about 80% confluent the next day. MDCKs were set up so as to be confluent on day 2 of the rescue. All tissue culture reagents were obtained from Gibco BRL and all plastic ware from Falcon Plastics.

Viruses

Stock viruses were passaged in 10-day-old embryonated eggs. After 48 h incubation, the allantoic fluids were harvested, clarified by centrifugation (4000 × *g* for 20 min at 4 °C) and stored in aliquots at −80 °C. Clinical isolates and all recombinant viruses were passaged in MDCK cells in serum-free medium containing 1 μg/ml trypsin.

Antibodies and reagents

A rabbit polyclonal antibody to A/Sydney/5/97, an H3N2 virus, was kindly provided by Dr. Maria Zambon (HPA, Colindale) and was used routinely to stain for H3 hemagglutinin. Goat anti-rabbit-FITC conjugate was obtained from Harlan Seralab and used at 1/100 dilution.

Cloning

RNA was extracted from allantoic fluid from infected eggs (Boom et al., 1990) and reverse transcribed using MMLV RT (Promega) and the RT primer (see Table 3). cDNA was amplified with Vent polymerase (NEB) using primers specific for segment 7 containing *Sap*1 restriction sites adjacent to the start of the noncoding regions, followed by a single round extension with Taq polymerase. Resulting fragments were TA cloned into a TOPO vector (Invitrogen PCR2.1) and then inserted into plasmid pPolIRTSapI. This vector was kindly provided by Dr. Thomas Zuercher (Glaxo-Smith-Kline) and has been previously described (Jackson et al., 2002). The *Sap*1 fragment was inserted such that human RNA polymerase I transcription produces an RNA subsequently cleaved by the ribozyme to precisely

Table 3
Primer sequences used for cloning and mutagenesis

Oligonucleotide primers used for cloning and manipulation		
Position 218	A to T (Udorn like)	5′ GGTGCAGGCGATGAGA**G**CCATTGGGACTCATCCTAG*CTCGAG*TG 3′ 5′ CA*CTCGAG*CTAGGATGAGTCCCAATGG**C**TCTCATCGCCTGCACC 3′ italics shows *Xho*I site, **G**/**C** is the base pair change
	T to A (WSN like)	5′ GGTGCAGGCAATGAGA**A**CCATTGGGACTCATCCTAG*CTCGAG*TG 3′ 5′CA*CTCGAG*CTAGGATGAGTCCCAATGGC**T**TCTCATTGCCTGCACC 3′ italics shows *Xho*I site, **A**/**T** is the base pair change
Position 95	R to K (WSN like)	5′GGGAATGG*C*GATCCAAATAACATGGACA**A**AGCAGTTAAACTGTATAG 3′ 5′ CTATACAGTTTAACTGCT**T**TGTCCATGTTATTTGGATC*G*CCATTCCC 3′ *C* removes a *Bst*Y1 site: **A**/**T** is the base pair change
	K to R (Udorn like)	5′GGGAACGG*C*GATCCAAATAACATGGACA**G**AGCAGTTAAACTGTATAGG 3′ 5′CCTATACAGTTTAACTGCT**C**TGTCCATGTTATTTGGATC*G*CCGTTCCC 3′ *C* removes a *Bst*Y1 site: **G**/**C** is the base pair change
Position 41	A to V (WSN like)	5′GCTGGAAAGAACACAGATCTTGAGG**T**TCTCATGGAATGGCTAAAG 3′ 5′CTTTAGCCATTCCATGAGA**A**CCTCAAGATCTGTGTTCTTTCCAGC 3′ **A**/**T** is the base pair change
	V to A (Udorn like)	5′GCAGGGAAGAACACCGATCTTGAGG**C**TCTCATGGAATGGCTAAAG 3′ 5′CTTTAGCCATTCCATGAGA**G**CCTCAAGATCGGTGTTCTTCCCTGC 3′ **C**/**G** is the base pair change
Overlap primers for making chimeras	UdM1WSNM2	5′GCGATTCAAGTGA**TCCTCTCGTC** 3′ 5′**GACGAGAGGA**TCACTTGAATCG 3′ bold indicates WSN M2 sequence
	WSNM1UdornM2	5′CGGATTCAGGTGA**CCCTCTTGTT** 3′ 5′**AACAAGAGGG**TCACTTGAATCG 3′ bold indicates Udorn M2 sequence
Segment seven termini	common for both WSN and Udorn	5′AGTCAT*GCTCTTC*GGCCAGCAAAAGCAGGTAGATATTG 3′ RT primer 5′AGTCAT*GCTCTTC*TATTAGTAGAAACAAGGTAG 3′ italics shows the *Sap*1 site used for cloning into the pPol1RT vector

represent a viral genomic segment 7 RNA. Chimeric cDNAs containing segment 7 sequences from A/Udorn/72 and A/WSN/33 were made by overlapping PCR. Two chimeras were produced. The first contained the Udorn M1 and the WSN M2 gene and the second contained WSN M1 and Udorn M2. These cDNAs were inserted into the pPol1RT vector for use in virus rescue. Mutations in the segment 7 cDNAs to alter the amino acid codons at residues 41, 95, and 218 were made using a Stratagene 'quick change' mutagenesis kit and appropriate primers (Table 3).

Virus rescue

Virus rescue was carried out using plasmids kindly provided by Dr. Thomas Zuercher (Glaxo-Smith-Kline). The set consisted of 12 plasmids: four expression plasmids with a CMV promoter, which direct expression of the proteins of the viral polymerase complex PB1, PB2, PA, and NP from strains A/Victoria/3/75. The remaining eight plasmids contain cDNA copies of viral RNAs derived from A/Victoria/3/75 inserted into the pPol1RT vector. The rescue method used was adapted from Neumann et al. (1999). Briefly, all 12 plasmids were transfected into 293T cells in 12-well plates using Fugene 6. Each time the rescue was carried out, a control of all 12 A/Victoria/3/75 plasmids was included and wild-type virus was always rescued from this experiment. To generate recombinant viruses, different cDNAs representing mutated segment 7 RNAs were substituted in place of the equivalent A/Victoria/3/75 segment 7 plasmid. After 24 h, the transfected cells were removed from the wells and mixed with MDCKs and co-cultured in 25-ml flasks. The first 6–8 h of the co-culture was carried out in 10% serum after which the cells (now firmly attached to the plastic) were washed briefly in serum-free media and the media replaced with serum-free media containing 2.5 μg trypsin/ml (Worthington). The flasks were examined on day 4 of the rescue (at which time cytopathic effect could be seen in the positive control flasks) and monitored daily thereafter. Supernatants containing recombinant viruses were harvested once the cell layers were completely destroyed by the virus. The harvested supernatants were spun at 4000 × *g* at 4 °C for 20 min to remove the cell debris and stored in aliquots at −80 °C. RT PCR was carried out on the supernatants of the recovered viruses and the amplified segment 7 cDNAs sequenced to confirm their genotype.

Plaque assays

Plaque assays were carried out in confluent monolayers of MDCK cells in 12-well plates. One hundred microliters of each of the dilutions of the virus to be assayed was applied to each well and incubated for 1 h. Cell layers were then washed in PBS before being overlaid with 0.6% agarose (Oxoid) in DMEM including 2 μg/ml trypsin (Worthington) and incubated at 34 °C. After 3 days, the agarose was removed and the cells stained with crystal violet dissolved in methanol and water. The anti-M2 antibody 14C2, used in the plaque reduction assay, was obtained from Professor R.A. Lamb and included in the overlay at a concentration of 3 μg/ml.

Microscopy

MDCK cells were grown on glass coverslips until completely confluent, infected at an MOI of approximately 0.1, and fixed 24 h after infection in 4% depolymerized paraformaldehyde in PBS (pH 7.0). Fixation was carried out on ice and the coverslips were then blocked in 5% BSA in PBS before being treated with the primary antibody. The stained coverslips were mounted in Vectorshield on glass slides, sealed with nail varnish, and imaging carried out on a Leica confocal microscope.

Cells were prepared for scanning electron microscopy (SEM) by growth on Melinex plastic coverslips obtained from Agar Scientific Ltd., cut into appropriate sized squares. Eighteen hours after infection, the coverslips were fixed in 4% depolymerized paraformaldehyde containing 1.5% glutaraldehyde, dehydrated through an acetone series, and critical point dried. Samples were sputtered with gold and examined on a LEO FEG scanning microscope.

Acknowledgments

We are grateful to Dr. Thomas Zurcher of Glaxo-Smith-Kline, Stevenage, UK, for providing the polI-RT and pHMG expression plasmids which allow rescue of A/Victoria/3/75 recombinant virus. We thank Maria Zambon, HPA, London, UK, for providing influenza isolates.

References

Boom, R., Sol, C.J., Salimans, M.M., Jansen, C.L., van Dillen, P.M.W., van der Noordaa, J., 1990. Rapid and simple method for purification of nucleic acids. J. Clin. Microbiol. 28, 495–503.

Bourmakina, S.V., Garcia-Sastre, A., 2003. Reverse genetics studies on the filamentous morphology of influenza A virus. J. Gen. Virol. 84, 517–527.

Brown, G., Rixon, H.W., Sugrue, R.J., 2002. Respiratory Syncytial Virus assembly occurs in GM1-rich regions of the host-cell membrane and alters the cellular distribution of tyrosine phosphorylated caveolin-1. J. Gen. Virol. 83 (8), 1841–1850.

Bucher, D.J., Kharitonenkow, L.G., Zakomiridin, J.A., Grivoriev, V.B., Klimenko, S.M., Davis, J.F., 1980. Incorporation of influenza M protein into liposomes. J. Virol. 36, 586–590.

Cox, J.C., Hampson, A.W., Hamilton, R.C., 1980. An immunofluorescence study of influenza virus filament formation. Arch. Virol. 63, 275–284.

Gomez-Puertas, P., Albo, C., Perez-Pastrana, E., Vivo, A., Portela, A., 2000. Influenza virus matrix protein is the major driving force in virus budding. J. Virol. 74 (24), 11538–11547.

Harris, A., Forouhar, F., Qui, S., Sha, B., Luo, M., 2001. The crystal structure of the influenza matrix protein M1 at neutral pH: M1–M1 protein interfaces can rotate in the oligomeric structures of M1. Virology 289, 34–44.

Hui, E.K.-W., Barman, S., Yang, T.Y., Nayak, D.P., 2003. Basic residues of

the helix six domain of influenza virus M1 involved in nuclear translocation of M1 can be replaced by PTAP and YPDL late assembly domain motifs. J. Virol. 77 (12), 7078–7092.

Inglis, S.C., Brown, C.M., 1981. Spliced and unspliced RNAs encoded by virion RNA segment 7 of influenza virus. Nucleic Acids Res. 9, 2727–2740.

Jackson, D., Cadman, A., Zurcher, T., Barclay, W.S., 2002. A reverse genetics approach for recovery of recombinant influenza B viruses from cDNA. J. Virol. 76 (22), 11744–11747.

Jin, H., Pleser, G., Zhang, J., Lamb, R.A., 1997. Influenza virus hemagglutinin and neuraminidase cytoplasmic tails control particle shape. EMBO J. 16 (6), 1236–1247.

Lamb, R.A., Choppin, P.W., 1981. Identification of a second protein (M2) encoded by RNA segment 7 of influenza virus. Virology 112, 729–737.

Latham, T., Galarza, J.M., 2001. Formation of wild-type and chimeric influenza virus-like particles following simultaneous expression of only four structural proteins. J. Virol. 75 (13), 6154–6165.

Liu, T., Muller, J., Ye, Z., 2002. Association of influenza virus matrix protein with ribonucleoproteins may control viral growth and morphology. Virology 304, 88–96.

Mitnaul, L.J., Castrucci, K.G., Murti, K.G., Kawaoka, Y., 1996. The cytoplasmic tail of influenza A virus neuraminidase (NA) affects NA incorporation into virions, virion morphology, and virulence in mice but is not essential for virus replication. J. Virol. 74, 8709–8719.

Neumann, G., Watanabe, T., Ito, H., Watanabe, S., Goto, G., Gao, P., Hughes, M., Perez, D., Donis, R., Hoffmann, E., Hobom, G., 1999. Generation of influenza A viruses entirely from cloned cDNAs. Proc. Natl. Acad. Sci. 96, 9345–9350.

Roberts, P.C., Compans, R.W., 1998. Host cell dependence of viral morphology. Proc. Natl. Acad. Sci. 95, 5746–5751.

Roberts, P.C., Lamb, R.A., Compans, R.W., 1998. The M1 and M2 proteins of influenza A virus are important determinants in filamentous particle formation. Virology 240, 127–137.

Sha, B., Luo, M., 1997. Structure of a bifunctional membrane-RNA binding protein, influenza virus matrix protein M1. Nat. Struct. Biol. 4 (3), 239–244.

Simpson-Holley, M., Ellis, D., Fisher, D., Macauley, J., Digard, P., 2002. A functional link between the actin cytoskeleton and lipid rafts during budding of filamentous influenza virions. Virology, 212–225.

Smirnov, Yu.A., Kuznetsova, M.A., Kaverin, N.V., 1991. The genetic aspects of influenza virus filamentous particle formation. Arch. Virol. 118, 279–284.

Wakefield, L., Brownlee, G., 1989. RNA-binding properties of influenza A virus matrix protein M1. Nucleic Acids Res. 17, 8569–8580.

Ward, A.C., 1995. Specific changes in the M1 protein during adaptation of influenza virus to mouse. Arch. Virol. 140 (2), 383–389.

Yao, Q., Compans, R.W., 2000. Filamentous particle formation by human parainfluenza virus type 2. J. Gen. Virol. 81 (5), 1305–1312.

Yasuda, J., Toyoda, M., Nakayama, M., Ishihama, A., 1993. Regulatory effects of matrix protein variations on influenza virus growth. Arch. Virol. 133, 283–294.

Yasuda, J., Bucher, D., Ishihama, A., 1994. Growth control of influenza A virus by M1 protein: analysis of transfectant viruses carrying the chimeric M gene. J. Virol. 68, 8141–8146.

Zebedee, S.L., Lamb, R.A., 1988. Influenza A virus M2 protein-monoclonal antibody restriction of virus growth and detection of M2 in virions. J. Virol. 62, 2762–2772.

Zebedee, S.L., Lamb, R.A., 1989. Growth restriction of influenza A virus by M2 protein antibody is genetically linked to the M1 protein. Proc. Natl. Acad. Sci. U.S.A. 86, 1061–1065.